ELSEVIER

Wear 193 (1996) 16–24

WEAR

Carbide tool wear mechanism in turning of Inconel 718 superalloy

Y.S. Liao, R.H. Shiue

Department of Mechanical Engineering, National Taiwan University, Taipei, Taiwan

Received 3 August 1994; accepted 21 March 1995

Abstract

Wear surfaces of the cutting tools are analyzed to study the wear mechanism of cemented carbide tools in turning of Inconel 718 superalloys. SEM and EPMA analyses indicated that the wear of carbide tools during high speed turning condition ($V = 35$ m min^{-1}) was caused by diffusion of elements (Ni or Fe) in workpiece into tool's binder (Co) by a grain boundary diffusion mechanism. This action weakened the bonding strength between carbide particles (WC, TiC, TaC) and the binder (Co). The carbide particles were then detached out of the cemented carbide tool by high flow stresses. The proposed grain boundary diffusion mechanism is also confirmed by theoretical analysis.

Keywords: Tool wear mechanism; Carbides; Superalloys; Grain boundary diffusion

1. Introduction

Inconel 718 is one kind of nickel–iron base superalloys. Owing to its superior high temperature mechanical properties such as resistance to oxidation and corrosion, high tensile stress and rupture stress, etc., it has been widely applied for the parts in aerospace industry and nuclear reactor. But, the combined effects of poor thermal properties, high temperature strength, tendency to severe work hardening, and high tool–workpiece affinity make machining of Inconel 718 very difficult because these properties result in high temperature, stress, and a thick adhering layer at the tool–work interface during machining [1].

The researches conducted so far for the machining of Inconel 718 are mainly focused on machining characteristics [2–4], and the appropriate tool material, geometry, and cutting conditions for economic machining [5,6]. Comparatively, very few have been done to identify tool wear mechanism during the machining of Inconel 718. Even though there are several studies on the machining of nickel base alloys by ceramics in recent years [7,8], carbide tools remained to be the main tool materials in machining this kind of material owing to their high toughness and low cost. Ham had conducted a series of cutting tests of Inconel 718 by C2 grade carbide [6], and he found that localized groove wear on side flank and chipping on the side cutting edge are the dominant causes of tool failure in some cases. But, in most cases, the tool wears uniformly and the flank wear progresses uniformly as cutting time increases up to the point where the tool fails. Based on the fractography of the tool surface after service, Focke et al. had concluded that abrasion wear plays the most important role on the wear of cutting tools in turning of Inconel 718 [9]. The groove wear on minor flank of cemented carbide tool in turning of pure nickel had been studied by Tan [10]. He found that temperature is the main driving force to cause tool wear. His proposal for tool wear mechanism is not different from carbide tool wear in machining of mild steels. Kramer and Suh proposed the solution wear theory which attributed the wear of carbide tool to the solubility of tool particles in material [11]. By observing the chip flow pattern, Wright and Chow concluded that the collapse of cutting edge in machining of nickel base alloys is mainly due to the increase of normal stress acting on the cutting edge [12]. All the studies stated above certainly contributed to the understanding of the failure of carbide tools in the machining of nickel base alloys. However, the investigations are not comprehensive. The proposal of Tan [10] is not quite true as the flow stress in machining Inconel 718 is high, and it is expected that this high stress would contribute to wear of the cutting tool. The study by Kramer and Suh [11] required more evidences to support their work as it is purely based on theoretical analysis. The "macro" approach of Wright and Chow [12] overlooked some pertinent information, besides, since the temperature in cutting of Inconel 718 is very high, other wear mechanisms besides abrasion wear are expected.

In this paper, the wear surfaces of cutting tools are investigated in detail using "micro" analysis, more evidences are given, and a new carbide tool wear mechanism in cutting of Inconel 718 is proposed.

SSDI 0043-1648(95)06644-6

2. Experiment

The experiments are carried out on a 7.5 hp engine lathe under semi-orthogonal, and dry cutting condition. The work material is Inconel 718 superalloy in either solid solution or aged state. Its chemical compositions are given in Table 1. The feed f and depth of cut d are 0.101 mm rev^{-1} and 1.5 mm, respectively, and they are not varied throughout the experiments. The cutting speed V is either 35 m min^{-1} (high speed) or 15 m min^{-1} (low speed). The total cutting time is 3 min. The tool materials are K20 and P20 carbides, respectively with the geometry of 0° inclination angle, 6° side rake angle, 0° approach angle, and 0.4 mm nose radius. The chemical compositions of tool materials are also given in Table 1. The cutting forces (principle force F_p, feed force F_q, and radial force F_r) are measured by the Kistler dynamometer. Since the turning process in the experiment can be considered as a plane strain and steady state condition, the radial force is neglected.

3. Results

The measured results for turning of aged Inconel 718 are summarized in Table 2. In the table, t_c is the chip thickness, a is the chip–tool contact length, VB and CR are flank wear length and crater wear depth. By incorporating these results with cutting mechanics [1], the average stresses in the primary and secondary deformation zones can be computed. The temperature in each deformation zone can then be estimated by using the moving heat source theory [1]. Mathematical expressions used to compute stresses and temperatures are summarized in Appendix A, and the computed results are given in Table 3. In the table, S_s and S_n denote shear and normal stresses, μ is the coefficient of friction. T_s and T_t are average temperatures in the primary and secondary deformation zones. From these tables, it is found that the flow stress (1.5–2.5 GPa) and temperature (800–1200 °C) in cutting of In718 are very high, and they are attributed to serious work hardening of In718 during turning.

The wear surface of the chip–tool interface of the K-type carbide tool is shown in Fig. 1. A sticking layer can be clearly seen. The sticking region which is very close to the cutting edge shows dimple-like ductile fractures (this particular region has the highest temperature, and is called seizure region). This phenomenon is quite different from that when mild steel is machined where the seizure region is smaller, and it is located at around $(1/2)a$ distance from the cutting edge (note: a is the chip–tool contact length). The occurrence of sticking region confirms the fact that high stresses and temperature are acting on the chip–tool interface. The same region has also been found in P-type carbide tool when it is used under the same turning conditions. When Inconel 718 is machined under a high speed cutting condition, it is also

Table 1
Chemical composition of work and tool materials

Materials	Specifications
Inconel	50–55% Ni, 0.08% C, 0.35% Mn, 18.5% Fe, 0.015% S, 0.35% Si, 0.3% Cu, 19% Cr, 3.05% Mo, 5.3% (Nb+Ta), 0.9% Ti, 0.5% Al, 0.95% B
K20 carbide	94% WC, 6% Co
P20 carbide	66.2% WC, 10.8% TaC, 12.8% TiC, 10.2% Co

Table 2
Measured results in machining of aged Inconel 718

Tool material	V (m min^{-1})	F_p (N)	F_q (N)	t_c (mm)	a (mm)	VB (μm min^{-1})	CR (μm min^{-1})	VB_{max} (μm)
P20	15	720	754	0.279	0.390	88.2	6.7	294
	35	780	617	0.191	0.210	134.0	16.2	777
K20	15	672	466	0.238	0.335	53.3	<1.0	160
	35	715	504	0.273	0.365	55.7	10.7	167

Table 3
Computed results in machining of aged Inconel 718

Tool material	V (m min^{-1})	Primary		Secondary		μ	T_s (°C)	T_t (°C)
		S_n (GPa)	S_s (GPa)	S_n (GPa)	S_s (GPa)			
P20	15	2.19	0.95	1.15	1.36	1.180	594	891
	35	2.90	1.23	2.35	2.11	0.896	779	1337
K20	15	1.83	1.13	1.28	1.01	0.788	642	467
	35	1.69	1.15	1.25	1.00	0.801	865	1047

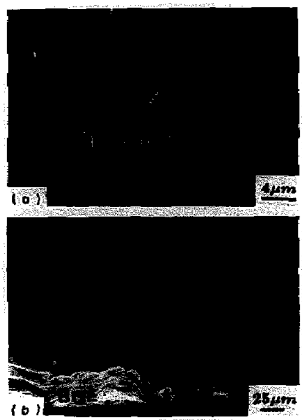

Fig. 1. Rake face of K20 carbide: (a) wear surface and (b) magnification of the area A (aged in 718, $V=35$ m min^{-1}; notations C.E. and C.F.D. in the photograph stand for cutting edge and chip flow direction).

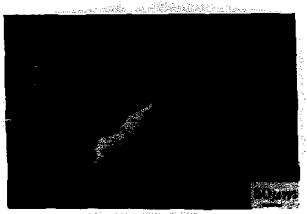

Fig. 2. Wear surface on the rake face near the nose radius: A, chipping; B, BUE (aged in 718, K20 carbide, $V=35$ m min^{-1}).

very often that a built up edge (BUE) would form at the cutting edge. Fig. 2 shows a wear surface of the rake face near the nose radius. From the figure, BUE and chipping of the cutting edge can be clearly seen. The occurrence of BUE implies that there is high chemical affinity due to high temperature existent on the chip–tool interface besides high stresses.

A typical wear surface on the flank face of K-type carbide is shown in Fig. 3(a) and Fig. 3(b). Similar to rake face, there is a large amount of sticking layer. When P-type carbide is used, the sticking layer can also be found, but comparatively, the wear is more irregular, the flank wear length is larger, and the groove is deeper. Inspecting the groove as that shown in Fig. 4(a) and Fig. 4(b), it can be seen that tool particles are subjected to high stresses which cause loss of large amount of Co and the local detachment of WC or (W,Ta,Ti)C from the base material. It is also noted that the flow stress could even be high enough to cause the fracture of tool particles (refer to that pointed by the arrow in Fig. 4(b)).

In order to study the fractography of the carbide tools on the chip–tool interface, the rake face of the cutting tool is hot

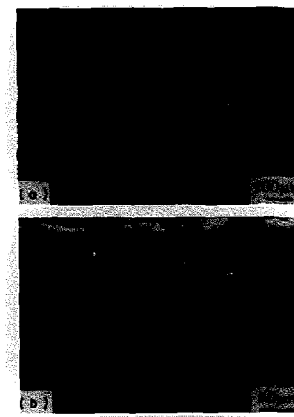

Fig. 3. Typical flank face: (a) wear surface and (b) magnification of the flank wear (solid sol. in 718, K20 carbide, $V=15$ m min^{-1}).

Fig. 4. Groove wear and its microstructure: (a) shape of the groove and (b) magnification of the area A (solid sol. in 718, P20 carbide, $V=35$ m min^{-1}).

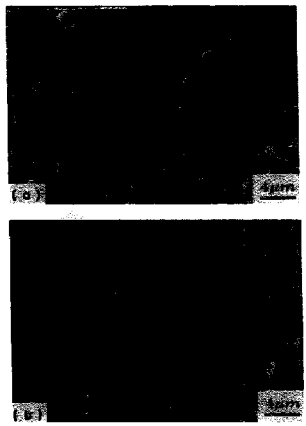

Fig. 5. Rake face of the new cutting tools after hot etching: (a) P20 carbide and (b) K20 carbide.

etched at 90 °C for 1 h using the 40 ml methyl + 40 ml HCl + 2 g $CuCl_2$ etching fluid. The thick sticking layer on the tool surface can be removed by this process. The surfaces of new P-20 and K-20 carbide tools are shown in Fig. 5(a) and Fig. 5(b), and those after the tools have been serviced for 3 min using high speed cutting condition ($V = 35$ m min^{-1}) are shown in Fig. 6(a) and Fig. 6(b). It can be seen from these figures that a large number of tool particles are detached from the tool surface for both P-type and K-type tools under high speed cutting conditions. Those tool particles remained on the surface are not distorted, broken, nor deformed.

When the particles on the tool surface before and after service are compared, it is noted that rounding of the particles takes place for both tools after service. There are two possible explanations for this result. Firstly, high flow stresses cause the originally multi-angles, irregular, and sharp tool particles to wear locally, and eventually the tool particles become rounded. If this conjecture is true, then all WC particles or (W,Ta,Ti)C particles should deform along a particular direction (i.e. chip flow direction). But, when Fig. 6(a) and Fig. 6(b) are examined, it is found that the tool particles are randomly distributed with no specific orientations on the tool surface. In addition, tool particles inside the tool surface show rounding characteristics as well. Hence, there is very slight possibility that high flow stresses play the principle role on rounding of the particles. Secondly, since the etching fluid for Inconel 718 does not react with WC nor (Ta,Ti,W)C of the tool particles, instead, it only reacts with the binder Co and Inconel 718 base material. Hence, if there is small amount of work material diffused into the cutting tool, and if the positions occupied by Co and the intermetallic phase between Co and WC or (W,Ta,Ti)C are replaced by this work material, then when the Inconel 718 etching fluid is applied, Co itself and intermetallic phase between Co and WC or (W,Ta,Ti)C would be etched away easily. This process will result in rounding of the tool particles. The above discussion also implies that diffusion and solubility phenomena had occurred between work and tool materials under high temperature conditions.

The line scan of EPMA is employed to analyze the concentration variations of W, Co and Ta of tool elements and Ni and Fe of work elements beneath the rake face. It is found that there is no conspicuous change of tool elements W, Co and Ta. But as shown in Fig. 7, there is evidence that work elements Ni and Fe had entered into the cutting tool. Fig. 8 shows similar result, but the evidence is less obvious due to a chip adherent to the tool face. Nevertheless, the more violent variation of the scanning line beneath the rake face as compared with that of the base line (to the right of the chip in Fig. 8) can still be vaguely seen. Because the temperature in the experiment is very high (about 1000 °C), hence, it is believed that the work materials entered into the cutting tool by ways of diffusion. Based on line scan, the diffusion distance for Ni or Fe is estimated, and it is larger than around 10^1 μm.

The quantitative analysis of the elements Ni and Fe beneath the rake face of the cutting tool by EPMA is shown in Fig. 9(a) and Fig. 9(b). From these figures it is realized that there are Ni and Fe at $> 10^1$ μm below the rake face. The EPMA Mapping (Fig. 10) also provides the evidence that

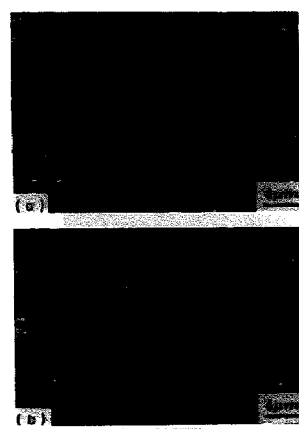

Fig. 6. Rake face of the used cutting tools after hot etching: (a) P20 carbide and (b) K20 carbide (aged in 718, $V = 35$ m min^{-1}).

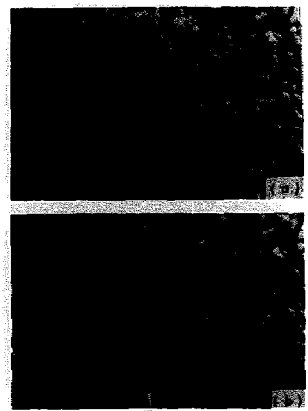

Fig. 7. EPMA line scan of work elements beneath the rake face of P20 carbide: (a) Ni and (b) Fe (aged In 718, $V=35$ m min^{-1}).

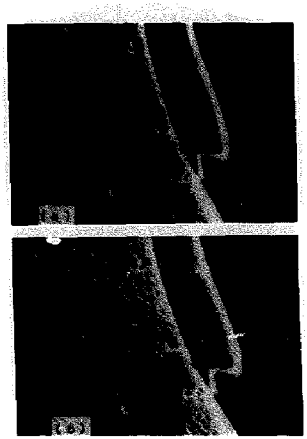

Fig. 8. EPMA line scan of work elements beneath the rake face of K20 carbide: (a) Ni and (b) Fe (aged In 718, $V=35$ m min^{-1}).

Ni and Fe are existent in the binder Co (Fig. 10(c), although the amount of Ni is small).

The back of the chip inspected by SEM is shown in Fig. 11(a). As pointed by the arrow, the tool particles embedded in the chip can be seen. Its compositions are analyzed by

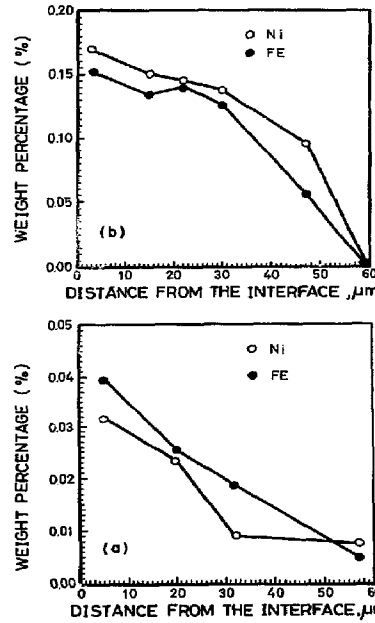

Fig. 9. Quantitative analysis of the work elements beneath the rake face: (a) P20 carbide and (b) K20 carbide.

EDAX, and the result is given in Fig. 11(b). These two figures provide another evidence that tool particles do detach from cutting tool during the cutting process.

4. Tool wear mechanism

From the experimental results presented in the previous section, the following inferences of carbide tool wear in machining of In718 may be drawn.

An apparent sticking layer formed on the tool face near cutting edge indicates that bonding between chip–tool interface had occurred. The bonding is likely originated from the driving force of very large stresses or high chemical affinity between tool and chip.

The fact of the rounding of tool particles and EPMA analyses had proved that elements of the work material had diffused into the tool, and these elements distributed around the

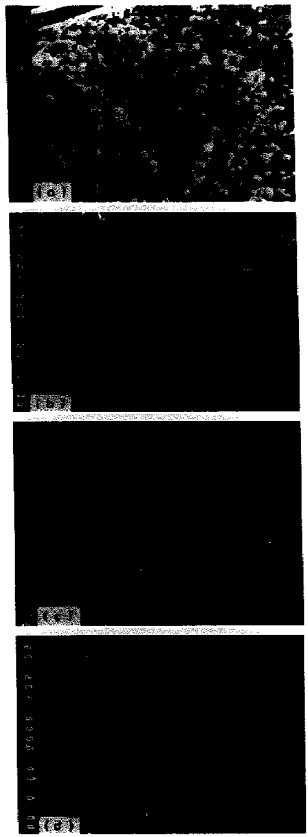

Fig. 10. (a) SEM of P20 tool's cross-section; (b) EPMA mapping of Co; (c) EPMA mapping of Ni, and (d) combination of (b) and (c).

binder Co and the intermetallic phases between carbides and binder.

The Co–Ni and Co–Fe phase diagrams show that Ni and Fe can be dissolved almost completely with Co at elevated temperatures [13]. This fact together with about 10% solubility of carbides in Ni and Fe at elevated temperature [11] implies that the tendency for work particles to diffuse into the binder is far larger than into tool particles. Hence, the assumption that the work materials had diffused into the binder is reasonable. The theoretical computation of diffusion distance had been carried out and it is given in Appendix B. The diffusion distance for the diffusion along the grain boundary at high temperature (> 1000 °C) is in the order of 10^1–10^3 μm, whilst that for bulk diffusion is 10^0–10^1 μm. Since from Figs. 7-9 it has been found that the work elements Ni and Fe distribute at $> 10^1$ μm below the rake face, it is concluded that Ni or Fe enters into the tool by ways of grain boundary diffusion, and it will distribute around the binder Co.

The rounding of tool particles (TiC, TaC, WC) in Fig. 6 also implies that the intermetallic phases of tool particles had dissolved at the existence of Ni around Co. The bonding between tool particles and Co would therefore be destroyed. It should be noted that the strength of Co itself would not be affected significantly by the presence of Ni around the grain boundary of Co. This is because the Co–Ni and Co–Fe phase diagrams have shown that Co and Ni (or Fe) can dissolve each other very well.

Since the bonding strength between tool particles and the binder had been destroyed, and there are high flow stresses during the cutting process, the tool particles will then be detached from tool surface. This is verified by Fig. 6. The wear resistance of the binder (Co) is very poor. Hence, when Co is exposed on the tool surface after the detachment of tool particles, the cutting tool will wear very rapidly. The solubility of titanium carbide in nickel is larger than that of tung-

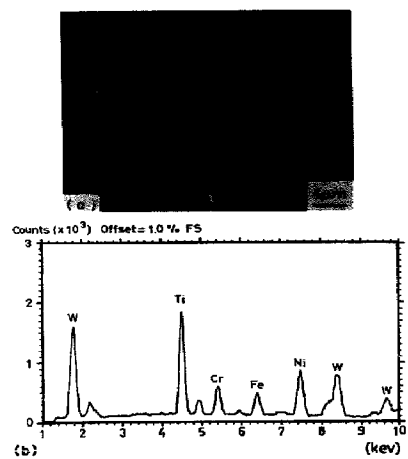

Fig. 11. The back of the chip: (a) photograph under SEM, and (b) composition analysis of complex carbides by EDAX.

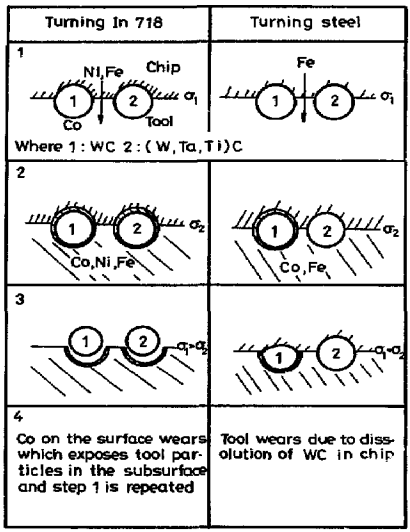

Fig. 12. Graphical illustration of carbide tool wear mechanisms in turning In 718 and steel.

sten carbide in nickel [11]. In addition, P-type carbide has a higher Co content (>10%) than that of K-type's (<6%). Hence, P-type carbide results in a far shorter tool life than K-type's in machining Inconel 718.

Based on the discussions described above, a tool wear mechanism for the use of carbide (either K-type of P-type) in turning of Inconel 718 is postulated as follows:

Step 1 Bonding between chip–tool interface is formed due to high stresses and temperature.

Step 2 Ni or Fe diffused into the Co grain boundaries, and the intermetallic phases between tool particles and binders by ways of grain boundary diffusion due to high temperature.

Step 3 The intermetallic phases are dissolved due to high affinity of tool particles with Ni. This process causes destruction of the bonding between tool particles and Co.

Step 4 When the bonding between tool particles and Co is less than that between tool particles and chip, large number of tool particles are detached from the tool. This is followed by rapid wear of Co, and step one is repeated.

The proposed wear mechanism is graphically illustrated in Fig. 12. When Inconel 718 is machined by carbide tools, bonding between chip–tool interface takes place first (step 1). This is followed by diffusion of Ni or Fe into Co grain boundary (step 2). In the third step, the intermetallic phases are dissolved. In the figure, particles 1 and 2 represent WC and (W,Ta,Ti)C, respectively, σ_1 is the bonding strength at chip–tool interface (i.e. flow stress), and σ_2 is the strength of Co (binder) on tool particles. When σ_1 is larger than σ_2, tool particles are detached from the cutting tool. The binder will then expose on the tool surface and wear away easily. Subsequently, the tool particles at subsurface appear on the tool surface, and the whole processes is repeated.

For comparison purpose, the use of same wear mechanism to explain carbide tool wear in machining of steels is also illustrated in the same figure. A few differences are noticed. Since the flow stress (0.1–0.5 GPa [13]) is not large enough (i.e. $\sigma_1 < \sigma_2$), tool wear is mainly due to dissolution of the surface of WC particles in chip [11,14] rather than detachment of WC particles from tool material. This can be confirmed when the wear surfaces obtained by Naerheim and Trent [14], and Wright and Chow [12] are examined; the surface is found to be comparatively more smooth, and there is no detachment of tool particles. The solubility of WC (K-type carbide) in iron is $\approx 2.6 \times 10^{-3}$ at 1600 °K, while it is $\approx 6.1 \times 10^{-3}$ for TiC (P-type carbide) in iron [11]. Since for P-type carbide, the solubility of TiC in iron is very small, there is very slight possibility for intermetallic phases to dissolve in iron. Hence, the TiC particles remain almost unchanged, and tool life is long.

5. Conclusion

A mixed type wear mechanism for turning of Inconel 718 by cemented carbide tool is postulated. At high cutting speed (in our case it is 35 m min^{-1}), the tool particles will diffuse into the binder (Co) by means of grain boundary diffusion. This mechanism weakens bonding strength between carbide tool particles and binder, and the tool particles are detached from base material under an extremely high flow stress (1–3 GPa). The postulated mechanism is confirmed by experimental results. Moreover, the mechanism is also applicable to interpret the wear of cemented carbide tool in machining of steels.

Appendix A. Equations to compute stresses and temperatures

For the orthogonal cutting, let V, t, b and α denote the cutting speed, undeformed chip thickness, depth of cut and the rake angle of the cutting tool. The quantities k, K and ρC are thermal conductivity, thermal diffusivity and volume specific heat of the work material. The output variables F_p and F_q are the principle and feed forces, ϕ is the shear angle, a is the chip–tool contact length, $r = t/t_c$ (t_c is the chip thickness). Then, the normal stress S_n and shear stress S_s and temperature T can be computed as follows: [1]

(i) Primary deformation zone:

$$S_n=\frac{(F_p\sin\phi+F_q\cos\phi)\sin\phi}{bt}$$

$$S_s=\frac{(F_p\cos\phi-F_q\sin\phi)\sin\phi}{bt}$$

$$T_s=\frac{R_1u_s}{J\rho_1C_1}+T_o$$

where $u_s=S_s\gamma$, and $\gamma=\tan(\phi-\alpha)+\cot\phi$, J is the energy–heat conversion factor, T_o is the ambient temperature, and $R_1=1/[1+1.328\sqrt{K_1\gamma/(Vt)}]$. The quantities k_1, K_1, and ρ_1C_1 are all evaluated at $(1/2)(T_s+T_o)$.

(ii) Secondary deformation zone:

If $F_c=F_p\sin\alpha+F_q\cos\alpha$, $B'=0.377q_2a/(k_2\sqrt{L_2})$, and $C'=q_2(aA/k_3)$, then

$$S_n=\frac{F_p\cos\alpha-F_q\sin\alpha}{ab}$$

$$S_s=\frac{F_c}{ab}$$

$$T_f=R_2B'+T_s$$

where $q_2=F_crV/Jab$, $L_2=0.25Var/K_2$, $R_2=(C'-T_s+T_o)/(B'+C')$, and

$$A=\frac{2}{\pi}\left[\ln\left(\frac{b}{a}\right)+\frac{2}{3}\left(\frac{a}{b}\right)+\frac{1}{2}\right]$$

The quantities k_2 and K_2 are thermal properties of work material, and k_3 is the thermal conductivity of the tool material. They are all evaluated at T_f.

In actual calculation of cutting temperatures, k_1 or k_2 is taken as a function of temperature, and it is equal to $10.7+8\times10^{-3}T$ [W m^{-1} K^{-1}], where T is in kelvins. The density of Inconel 718 is 8.21 mg m^{-3}, and C is 0.104. For tool material, k_3 is 100 for K20 carbide, and it is 50 for P20 carbide.

Appendix B. Theoretical analysis

The diffusion concentration denoted by c at a position of coordinate (x, y) under grain boundary diffusion can be written as [15]:

$$c(x,y,t)=C_o\exp\left[\frac{-y\sqrt{2}}{(\pi D_lt)^{1/4}(\delta D_b/D_l)^{1/2}}\right]\left[1-\mathrm{erf}\left(\frac{x}{2\sqrt{D_lt}}\right)\right] \quad \text{(B1)}$$

where C_o is a constant, D_l is lattice diffusivity in cm^2 s^{-1}, D_b is grain boundary diffusivity, δ is sheet thickness where diffusion takes place (≈4 Å), and t is time. If R is gas constant, and T is temperature in kelvins, then diffusivities D_b and D_l can be expressed as

$$D_b=D_{ob}\exp\left(-\frac{Q_{ob}}{RT}\right) \quad \text{(B2)}$$

$$D_l=D_{ol}\exp\left(-\frac{Q_{ol}}{RT}\right) \quad \text{(B3)}$$

The parameters D_{ob}, D_{ol}, Q_{ob} and Q_{ol} for Ni and Fe are given in Table 4.

If β is defined as

$$\beta=\frac{D_b\delta}{2D_l\sqrt{D_lt}} \quad \text{(B4)}$$

Table 4
Numerical values of D_{ol}, D_{ob}, Q_{ol} and Q_{ob} for Ni and Fe

Element	D_{ol} (cm^2 s^{-1})	D_{ob} (cm^2 s^{-1})	Q_{ol} (kcal mol^{-1})	Q_{ob} (kcal mol^{-1})
Ni	1.9	0.031	68.0	25.6
Fe	18	8.8	64.0	40.0

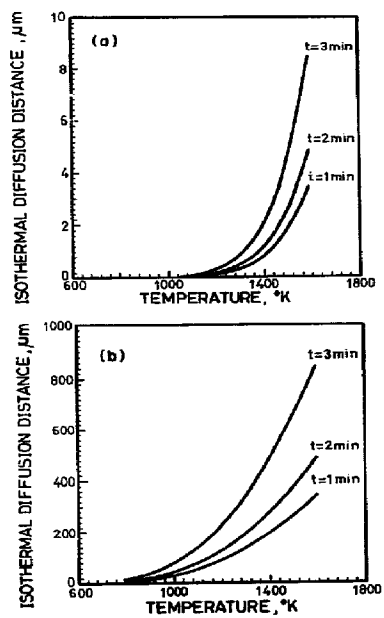

Fig. 12. Theoretical isothermal diffusion distance of Ni: (a) bulk diffusion and (b) grain boundary diffusion.

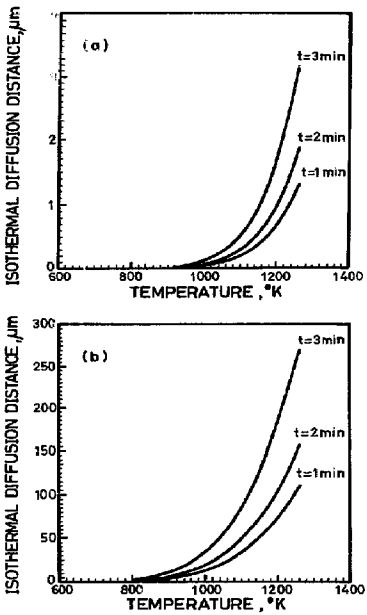

Fig. 14. Theoretical isothermal diffusion distance of Fe: (a) bulk diffusion and (b) grain boundary diffusion.

then, it had been proved that grain boundary diffusion is the main way for atomic diffusion when $\beta > 1.0$ [16]. By substituting Eq. B2 and Eq. B3 into Eq. B4, it can be found that grain boundary diffusion for Ni and Fe becomes important at temperatures of 1250 °C and 980 °C respectively. The maximum diffusion distance under grain boundary diffusion for Ni or Fe atoms can be estimated by applying isothermal diffusion theory. The theoretical diffusion distance can be expressed as

$$X = \sqrt{2\bar{D}t} \qquad \text{(B5)}$$

where in the above equation, X is the diffusion distance in μm, $\bar{D}$ is the diffusivity in $\mu m^2 s^{-1}$, and t is the diffusion time (in our case, it is the cutting time in seconds). Substituting D_b and D_l for Ni and Fe into Eq. B5, the theoretical diffusion distances for Ni and Fe at various cutting times can be drawn, and they are given in Fig. 13 and Fig. 14. From these figures, it can be seen that the diffusion distance by means of grain boundary diffusion at high temperatures (> 1000 °C) is around 10^1–10^3 μm, while for bulk diffusion it is around 10^0–10^1 μm. There is significant difference in terms of the order of the diffusion distance for two kinds of diffusions.

References

[1] M.C. Shaw, *Metal Cutting Principles*, Clarendon Press, Oxford, 1984.
[2] N. Zlatin and J. Christopher, Machining characteristics of difficult to machine material, in V.A. Tipnis (ed.), *Influence of Metallurgy on Machinability*, ASM, 1975, pp. 296–307.
[3] H.R. Conaway, Machining the high-nickel alloys, in V.A. Tipnis (ed.), *Influence of Metallurgy on Machinability*, ASM, 1975, pp. 247–256.
[4] R. Komanduri and T.A. Schroeder, On shear instability in machining a nickel–iron base superalloy, *Trans. ASME, J. Eng. Ind.*, *108* (1986) 90–100.
[5] E.C. Orth and S. Ebenhoch, Machining work-hardening metals, *Carbide Tool J.*, *15* (1983) 3–7.
[6] I. Ham Computerized machinability study for Inconel-718, in V.A. Tipnis (ed.), *Influence of Metallurgy on Machinability*, ASM, 1975, pp. 324–346.
[7] N. Narutaki, Y. Yamane, K. Hayashi and T. Kitagawa, High speed machining of Inconel 718 with ceramic tools, *Ann. CIRP*, *42* (1) (1993) 103–106.
[8] J. Vigneau and P. Bordel, Influence of the microstructure of the composite ceramic tools on their performance, *Ann. CIRP*, *36* (1) (1987) 13–16.
[9] A.E. Focke, F.E. Westermann, J. Kemphaus, W.T. Shin and M. Hoch, Wear of superhard materials when cutting superalloys, in *Wear of Materials*, ASME, 1977, pp. 228–237.
[10] M.T. Tan, Groove wear of tools in NC turning of pure nickel, *Ann. CIRP*, *35* (1) (1986) 71–74.
[11] B.M. Kramer and N.P. Suh, Tool wear by solution: a quantitative understanding, *Trans. ASME, J. Eng. Ind.*, *102* (1980) 303–309.
[12] P.K. Wright and J.C. Chow, Deformation characteristics of nickel alloys during machining, *Trans. ASME, J. Eng. for Industry*, *104* (1982) 85–93.
[13] J.L. Murray, H.B. Lawrence and B. Hugh, *Binary Alloy Phase Diagrams*, ASM, 1986.
[14] Y. Naerheim and E.M. Trent, Diffusion wear of cemented carbide tools when cutting steel at high speeds, *Metals Tech.*, (1977) 548–556.
[15] J.C. Fisher, Calculation of diffusion penetration curves for surface and grain boundary diffusion, *J. Appl. Phys.*, *22* (1) (1951) 74–77.
[16] P.G. Shewmon, *Diffusion in Solids*, McGraw-Hill, 1972.